

# Airborne and satellite observations of volcanic ash from the Eyjafjallajökull eruption

Stuart M. Newman<sup>1</sup>, Lieven Clarisse<sup>2</sup>, Daniel Hurtmans<sup>2</sup>, Franco Marenco<sup>1</sup>, Ben Johnson<sup>1</sup>, Kate Turnbull<sup>1</sup>, Stephan Havemann<sup>1</sup>, Anthony J. Baran<sup>1</sup>, Debbie O'Sullivan<sup>1</sup> and Jim Haywood<sup>1,3</sup>

<sup>1</sup>Met Office, FitzRoy Road, Exeter EX1 3PB, United Kingdom

<sup>2</sup>Spectroscopie de l'Atmosphère, Service de Chimie Quantique et Photoscopique, Université Libre de Bruxelles (ULB), Brussels, Belgium

<sup>3</sup>College of Engineering, Mathematics, and Physical Science, University of Exeter, Exeter, Devon, United Kingdom.

## Abstract

An extensive set of airborne and satellite observations of volcanic ash from the Eyjafjallajökull Icelandic eruption are analyzed for a case study on 17 May 2010. Data collected from particle scattering probes and backscatter lidar on the Facility for Airborne Atmospheric Measurements (FAAM) BAe 146 aircraft allow estimates of ash concentration to be derived. Using radiative transfer simulations we show that airborne and satellite infrared radiances can be accurately modeled based on the in situ measured size distribution and a mineral dust refractive index. Retrievals of ash mass column loading using Infrared Atmospheric Sounding Interferometer (IASI) observations are shown to be in accord with lidar-derived mass estimates, giving for the first time an independent verification of a hyperspectral ash variational retrieval method.

## 1. Introduction

The eruption of the Eyjafjallajökull Icelandic volcano in April-May 2010 caused widespread disruption to European air traffic. This was due to the transport of volcanic ash particles over much of Europe, which are known to damage jet engines if encountered at high concentrations (Guffanti et al., 2010; Witham et al., 2007). As well as highlighting the importance of satellite data in ash detection and monitoring, the incident motivated further research into the quantitative retrieval of ash concentrations from space.

A new generation of spaceborne hyperspectral sounders, such as the Atmospheric Infrared Sounder (AIRS) on the Aqua platform and the Infrared Atmospheric Sounding Interferometer (IASI) on MetOp, offer greater information content than conventional multi-channel sounders. The very high spectral resolution from hyperspectral

measurements has proven to be valuable in monitoring and tracking the evolution of SO<sub>2</sub> from large volcanic eruptions which can be used to validate numerical model simulations (e.g. Haywood et al., 2010). The unique signature of volcanic ash in hyperspectral data allows parameters such as aerosol effective radius, concentration and mass to be retrieved with greater confidence than if only a few wavelengths are used (Clarisse et al., 2010a; Prata et al., 2010).

The UK Facility for Airborne Atmospheric Measurements (FAAM) BAe-146 research aircraft made a total of twelve flights dedicated to remote sensing and in-situ measurements of volcanic ash (Johnson et al., 2012). The reader is referred to Marenco et al. (2011) for a description of the downward-looking Leosphere ALS450 elastic backscatter lidar measurements, and the corresponding data analysis required to obtain quantitative estimates of ash size distribution, optical extinction and mass loading. Turnbull et al. (2012) discuss the in situ airborne observations on 17 May 2010 obtained from the FAAM BAe-146 and Deutsches Zentrum für Luft- und Raumfahrt (DLR) Falcon aircraft which constitutes the case study explored in this paper. Here we seek to demonstrate radiative closure between (a) the radiation observations; (b) collocated profiles of aerosol extinction derived from lidar backscatter measurements; (c) aerosol optical properties based on a representative particle size distribution and choice of ash complex refractive index; and (d) radiative transfer simulations. Further, we test the performance of hyperspectral retrievals of ash mass loadings using IASI observations, providing independent verification of such methods for the first time.

## 2. Modeling

We adopt the spherical assumption of particle shape for calculating infrared optical properties via Mie-Lorenz theory using the mineral dust refractive index of Balkanski et al. (2007). By way of justification for this, the scalar optical properties (i.e., extinction cross-section, single scattering albedo  $\omega_0$  and asymmetry parameter  $g$ ) calculated assuming equal volume spheres have been compared against exact T-matrix (Havemann and Baran, 2001) calculations assuming randomly oriented hexagonal columns of aspect ratio unity (ratio of length-to-diameter) at three wavelengths (8.2  $\mu\text{m}$ , 9.8  $\mu\text{m}$  and 11.0  $\mu\text{m}$ ). The results of comparing the Mie-Lorenz calculations against T-matrix show that the extinction cross-section,  $\omega_0$  and  $g$  are generally within 10%, 2% and <1% respectively of the exact calculations.

We require an aerosol particle size distribution (PSD) to generate the optical properties. On the FAAM aircraft the Passive Cavity Aerosol Spectrometer Probe (PCASP, covering size bins in the range 0.1-3.0  $\mu\text{m}$ ) and the University of Manchester's Cloud and Aerosol

Spectrometer (CAS, 0.5–50  $\mu\text{m}$ ) collected data which have been processed to derive a representative PSD for this event (Johnson et al., 2012). We apply the optical properties calculated using Mie-Lorenz theory to full scattering calculations covering the range of wavelengths to which the FAAM BAe-146 remote sensing instrumentation is sensitive. We distinguish between the shortwave solar spectrum and the thermal infrared region. For the shortwave data analysis the reader is referred to Newman et al. (2012). For the modeling of radiances over the mid-infrared spectral range we make use of the Havemann-Taylor Fast Radiative Transfer Code (HTFRTC) which has been developed at the Met Office as a fast forward model and 1-dimensional variational inverse model. The use of principal components as a basis in HTFRTC, in contrast to line-by-line calculations, permits accurate and efficient computation (Liu et al., 2006; Havemann, 2006). More recently, scattering has been incorporated which allows the simulation of cloud and aerosol scenes as well as clear sky profiles (Havemann et al., 2008). We initialize HTFRTC with profiles of temperature and humidity from dropsonde observations, an ozone concentration profile from FAAM BAe-146 in situ measurements and vertical extinction profiles from the airborne lidar. HTFRTC does not currently include absorption due to  $\text{SO}_2$  which we neglect (we have demonstrated, not shown, that the quantities of  $\text{SO}_2$  detected by the FAAM instrumentation have negligible impact on the results we show here). We also require an estimate of sea surface temperature (SST) which we choose for consistency with ARIES downwards-looking radiances at the lowest available altitude over the southern North Sea (284.0 K).

### **3. Aircraft remote sensing measurements: ARIES infrared radiances**

The Airborne Research Interferometer Evaluation System (ARIES) (Wilson et al., 1999) measures infrared radiances over two spectral bands between 550–3000  $\text{cm}^{-1}$  (18–3.3  $\mu\text{m}$ ) at 1  $\text{cm}^{-1}$  resolution. It is capable of scanning vertically upwards and a number of view angles cross-track downwards. The infrared spectrum is particularly sensitive to the presence of ash in the window region between approximately 770–1250  $\text{cm}^{-1}$ . Analysis of ARIES spectra recorded during the Eyjafjallajökull eruption episode in April/May 2010 showed a very straightforward correlation between the brightness temperature slope in micro-windows between 1130–1250  $\text{cm}^{-1}$  and the presence of ash in the field of view. (By micro-windows we mean ARIES spectral channels with a clear sky transmittance close to unity.) Note that this spectral slope method is very similar in practice to calculating a brightness temperature difference for two channels, such as for 1231.5 and 1168  $\text{cm}^{-1}$  described by Clarisse et al. (2010b), although the calculation of a slope using multiple channels does assist in reducing the impact of instrument noise for any particular channel. Clarisse et al. demonstrated even better performance for a spectral shape correlation method, particularly for the discrimination of ash from desert dust; however,

we find for this case study that the spectral slope gives adequate information for ARIES ash detection.

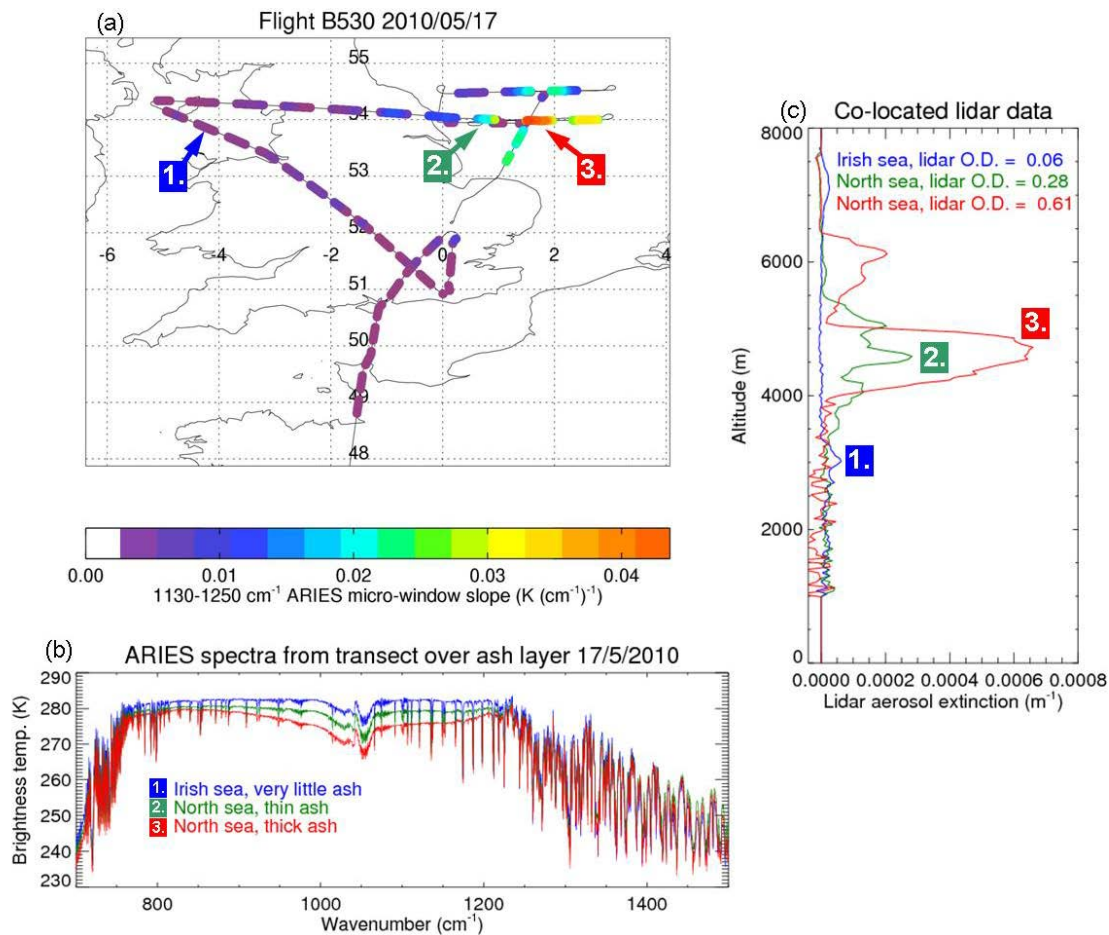


**Figure 1.** (a) Flight track of the FAAM BAe 146 aircraft on 17 May 2010. The track is overlaid with color-coded ARIES observations of the brightness temperature slope for micro-windows in the range 1130-1250 cm<sup>-1</sup>. The labels 1, 2, 3 denote the locations of representative low, medium and high ash loadings respectively. (b) ARIES downward-looking brightness temperature spectra for the three selected locations above the ash layer, spanning the mid-infrared atmospheric window region. (c) Lidar extinction profiles collocated with the three selected ARIES observations, with total AOD in the range 0.06 to 0.61 (see legend).

The derived brightness temperature slope for ARIES data collected on 17 May 2010 is shown in Figure 1 (a). For the early part of the flight over southern England and the Irish Sea the slope is consistently close to zero, despite considerable variations in the expected infrared surface emissivity and variable cloud amounts detected by the lidar. This finding

gives confidence that the simple slope diagnostic is not overly prone to false-positive identifications of ash. The later part of the flight over the North Sea encountered much higher aerosol concentrations (as detected by the lidar) with a concomitant increase in the ARIES slope diagnostic. The position of the maximum ash detection values correlates well with other observations of the peak plume concentrations, e.g. the SEVIRI satellite imagery shown in Figure 2.

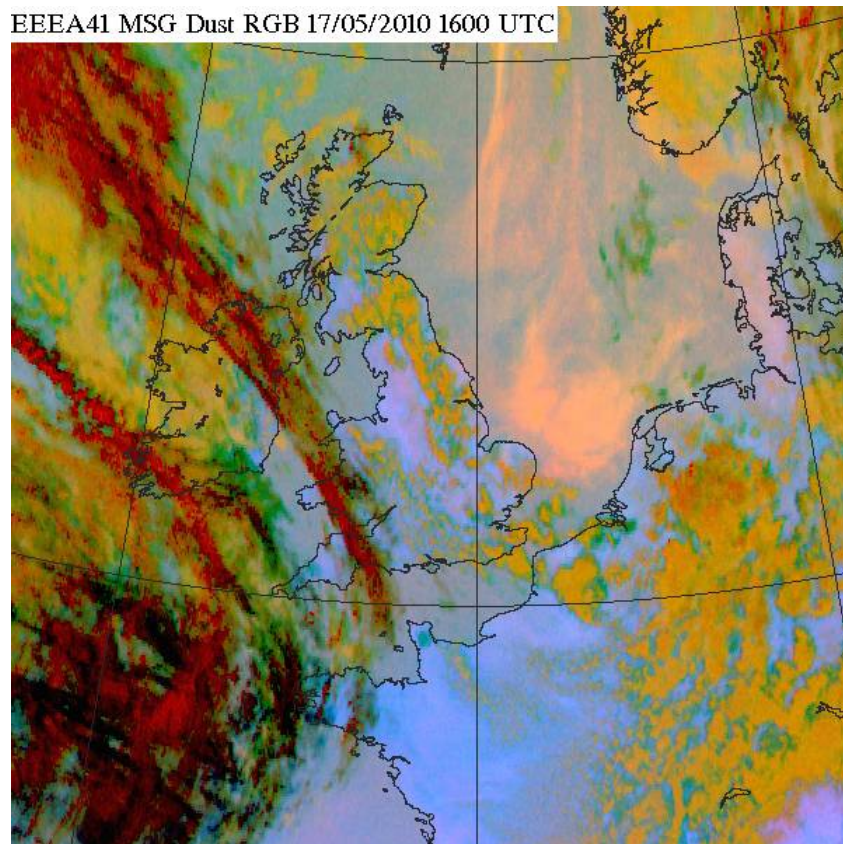
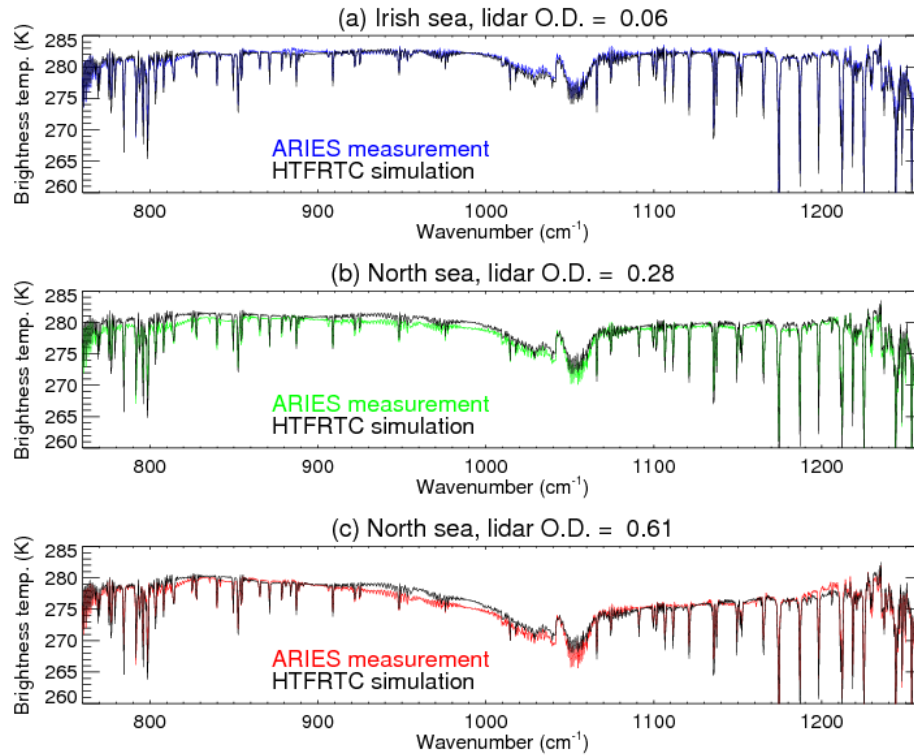


**Figure 2.** Red-green-blue (RGB) dust identification product developed at the Met Office using SEVIRI channel combinations. The area around Britain and Ireland and parts of western Europe is shown, valid at 1600 UTC on 17 May 2010. The bright pink features in the North Sea are indicative of volcanic ash.

For ease of analysis a subset of the data has been selected based on lidar inferred aerosol optical depth (AOD) values. AODs are calculated from the altitude below which the identified ash signature is negligible up to the aircraft altitude. Figure 1 (a) shows three subset locations corresponding to (1) very low AOD over the Irish Sea, (2) intermediate AOD close to the coast over the southern North Sea, and (3) high AOD further east over

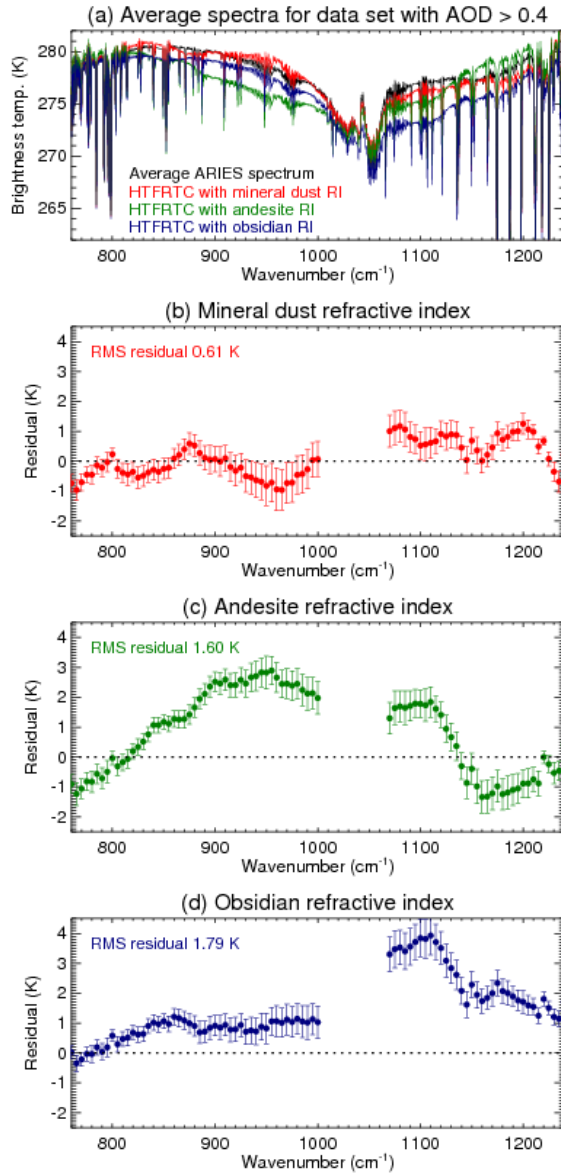
the southern North Sea. The respective ARIES brightness temperatures and lidar extinction profiles for these locations are shown in Figure 1 (b, c). The ARIES brightness temperature depression in the 770–1250  $\text{cm}^{-1}$  range due to the presence of ash is clearly observed. The sample locations were carefully selected to be free of cloud based on examination of lidar backscatter returns.

Figure 3 shows the results of HTFRTC simulations across the mid-infrared window region, taking as input the dropsonde-measured atmospheric temperature and humidity profile and the collocated lidar aerosol extinction profile for each of the three test locations, compared with ARIES observations. Optical properties derived using the Balkanski et al. (2007) mineral dust refractive index have been used in the simulations. The aerosol signal is seen as a broad depression in brightness temperature with maximum impact around 1000-1100  $\text{cm}^{-1}$ . The agreement of simulations with measurements is generally good over the range of AOD studied here, giving confidence that optical properties such as these can be used to derive quantitative estimates of ash loading from hyperspectral satellite instruments (see Section 4).



**Figure 3.** ARIES brightness temperatures overlaid with HTFRTC simulations for three examples of ash optical thickness in the down-looking scene (cf. Figure 1). The collocated lidar extinction profile has been used as input to the simulation in each case. (a) Lidar AOD of 0.06; (b) AOD of 0.28; (c) AOD of 0.61.

It is important to note that the ash spectral signature is sensitive to the specific composition (and therefore aerosol complex refractive index) and grain size as documented for a number of volcanic eruptions by Clarisse et al. (2010b). To investigate further we generate optical properties based not only on the refractive index of mineral dust (Balkanski et al., 2007), but also volcanic materials andesite and obsidian (both tabulated by Pollack et al. (1973)). Obs-calc residuals for ARIES using the three data sets are shown in Figure 4. Not only are the root mean square (RMS) residuals significantly smaller when using the refractive indices of Balkanski et al., (2007) compared to the other choices, the spectral shape of the ash signature is markedly different for the various indices. Optical properties based on andesite and obsidian are a poor fit to the ARIES observations, leading to residuals of 3-4 K at some frequencies.



**Figure 4.** (a) Average ARIES brightness temperature spectrum (black) for scenes where the lidar AOD was above a threshold of 0.4. Also plotted are HTFRTC simulations based on different assumed refractive indices: mineral dust (Balkanski et al., 2007) in red; andesite (Pollack et al., 1973) in green; obsidian (Pollack et al., 1973) in blue. (b)-(d) Observed-calculated brightness temperature residuals for each refractive index data set.

#### 4. IASI observations and retrievals

The Infrared Atmospheric Sounding Interferometer (IASI) is a high resolution infrared sounder onboard Metop-A which measures the Earth's outgoing radiation twice a day globally with a 12 km diameter footprint at nadir. The spectrometer has a wide spectral coverage 645-2760  $\text{cm}^{-1}$  with a medium to high spectral resolution (0.5  $\text{cm}^{-1}$  apodized, sampled at 0.25  $\text{cm}^{-1}$ ) (Clerbaux et al., 2009).

Recently, a radiative transfer code has been developed for the retrieval of trace gases and aerosols from observed spectra (Clarisse et al., 2010a) of which the most important aspects are summarized here. Its forward model is based on a spherical layer model of the atmosphere and uses a doubling-adding routine (supporting an arbitrary number of streams) to deal with the effects of multiple scattering on aerosols. The retrieval is based on the optimal estimation approach, and can be used to simultaneously retrieve both trace gas concentrations and aerosol loadings and effective radii. Unlike other codes, it does not rely on two step retrievals, lookup tables or the use of micro-windows.

In order to retrieve aerosol properties accurately (total mass and effective radius), there are two important prerequisites. The first is good knowledge of the size distribution (type and width), while the second is a good knowledge of the refractive index of the measured aerosol. If the assumed refractive index does not exhibit the same spectral features as the observed spectra the optimal estimation iteration is unlikely to converge (or convergence is only possible when taking into account an unrealistically high instrumental noise, as we will demonstrate herewith). Other less important factors that affect the accuracy of the retrieval are the assumed aerosol altitude, layer thickness, surface temperature and instrumental noise.

Figure 5 shows (in blue) part of a measured IASI spectrum observed around 11.27 UTC on 17 May above the North Sea (54.79N, 0.69E). A distinct V-shape absorption feature can be distinguished between 800 and 1235  $\text{cm}^{-1}$  which is characteristic of the presence of mineral aerosols (DeSouza-Machado et al., 2006) (not to be confused with the ozone absorption around 1050  $\text{cm}^{-1}$ , here shown in the gray shaded rectangle). A comparison with Figure 3 shows that essentially the same ash spectral signature is seen in both the ARIES and IASI observations.

For the synthetic reconstruction (shown in red) we have used the size distribution as determined from in situ CAS and PCASP measurements from the FAAM aircraft, while the assumed refractive indices were taken from Balkanski et al. (2007) corresponding to desert dust with a 1.5% hematite content.. The layer height (5 km) and thickness (1.5 km) used in the retrieval were idealized based on the set of lidar extinction profiles retrieved

for this date. The surface temperature was taken from the IASI level 2 products as disseminated by EumetCast. The remaining parameters (total aerosol loading, humidity, ozone profiles and SO<sub>2</sub> total columns) were treated as unknown and constitute the retrieved properties. As can be seen from the residual (light green) in Figure 5, the fit is good throughout the fitting region, and captures the large scale absorption in the atmospheric window; it does, however, miss out on some of the finer features. This manifests itself also in the RMS of the residual which is about twice IASI's instrumental noise. Also shown in Figure 5 is a reconstruction of how the observed spectrum would have looked (pink) without the aerosol contribution (residual in dark green).

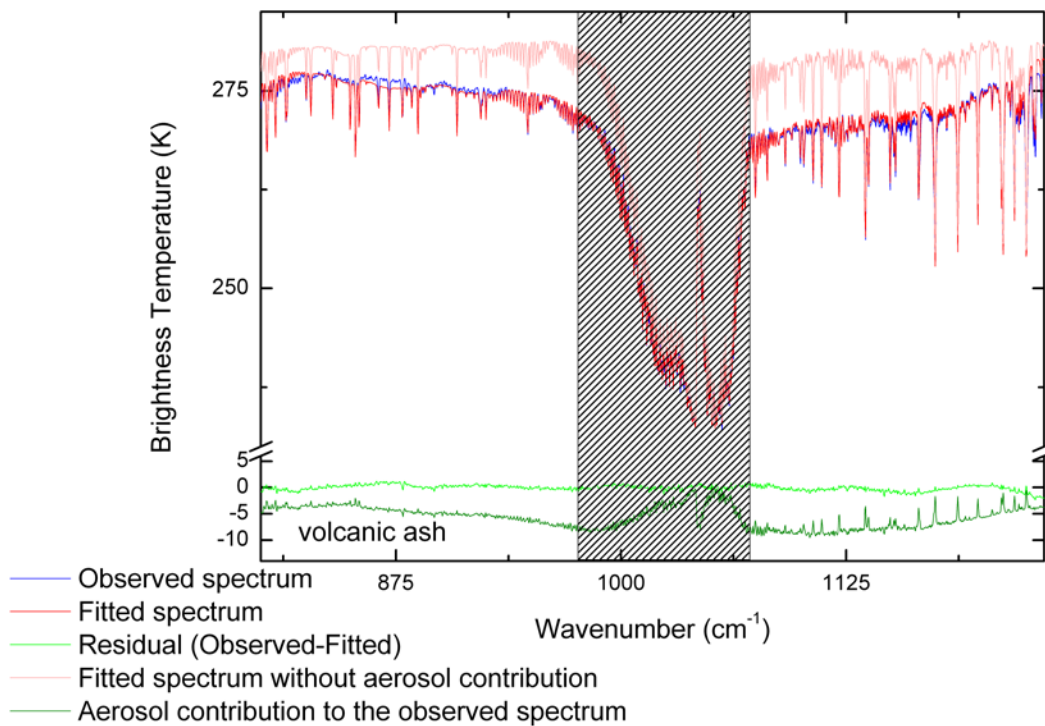


**Figure 5.** Example IASI observation and fit (measured brightness temperature spectra and residuals, see legend).

Traditionally, ash retrievals of infrared spectra use one of three sets (andesite, basalt or obsidian) of refractive indices obtained by Pollack et al. (1973) from optical measurements on slices of rock samples. The optical properties of rock are arguably very different from airborne particles. Unfortunately, there have been almost no measurements of refractive indices of volcanic ash (as aerosol) and those that were reported were measured at visible and ultraviolet wavelengths (e.g. Patterson et al. (1983)). In many

cases the refractive index data of Pollack have been used in the retrieval of mass loadings from infrared broadband instruments (e.g. Pavolonis et al., 2009; Stohl et al., 2011).

We have used refractive indices of Balkanski et al. (2007) because the fits obtained with these indices are better than any of the other refractive indices we have tried. This is in spite of the fact that the refractive indices were calculated to represent the refractive index of windblown sand from desert regions (Sahara, Arabian and Gobi). The residuals of six fits with differing refractive indices are shown in Figure 6. For the mineral dust refractive indices of Balkanski et al. and the obsidian refractive indices IASI's instrumental noise was set at  $3 \times 10^{-6} \text{ W m}^{-2} \text{ m sr}^{-1}$ , close to real instrumental noise. For the other indices this led to diverging fits; we therefore needed to use a larger virtual noise of  $1.3 \times 10^{-5} \text{ W m}^{-2} \text{ m sr}^{-1}$  to make the fits converge. Using different refractive indices has a considerable effect on total retrieved masses, up to 100% between the lowest and highest values. Future experimental measurements leading to new, independent and public data sets of refractive indices of different types of volcanic ash would therefore be highly desirable.

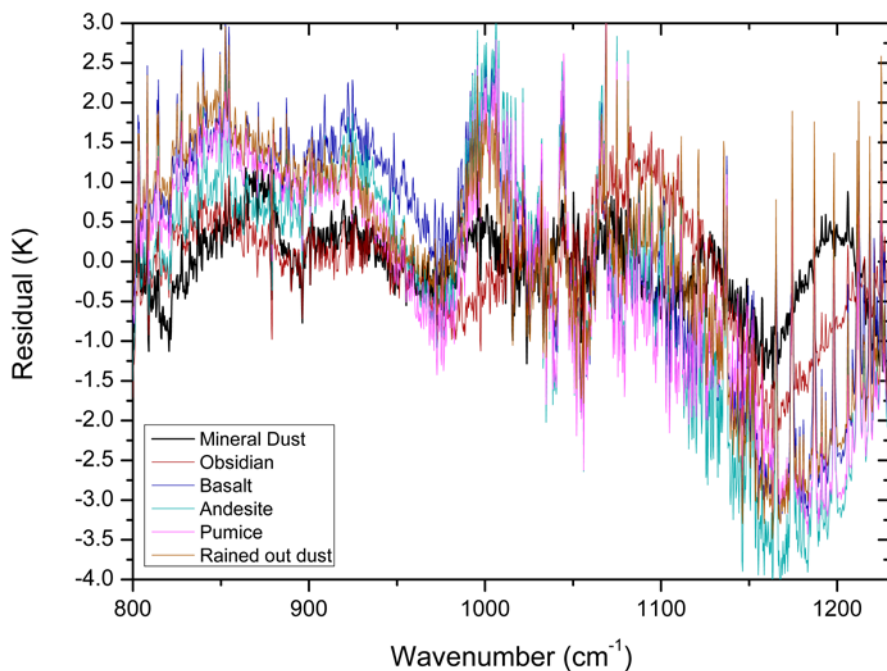


**Figure 6.** Residuals of the same fit as in Figure 5 but with different refractive indices (see legend).

We have performed the retrievals as in Figure 5 for all spectra measured on the 17 May 2010 above Northern Europe and the North Sea which passed the ash correlation

detection test (Clarisse et al., 2010b). The results are summarized in Figure 7. The largest values were found to be  $2.5\text{g/m}^2$  while total masses were 370 and 300 kT respectively for the morning and evening orbit. It is instructive to compare IASI retrievals of mass loading with those derived from other sources, particularly from the lidar data recorded during the period 14:15 to 16:30 UTC on 17 May 2010. This period occurs mid-way between the IASI morning and evening overpass times. We can select IASI fields of view (FOVs) which relate approximately to the same area of the ash cloud as the lidar returns (estimated, based on SEVIRI-observed advection of the ash plume with time). However, we note that this analysis cannot account for variations in the ash distribution that deviate from a simple translation of position.

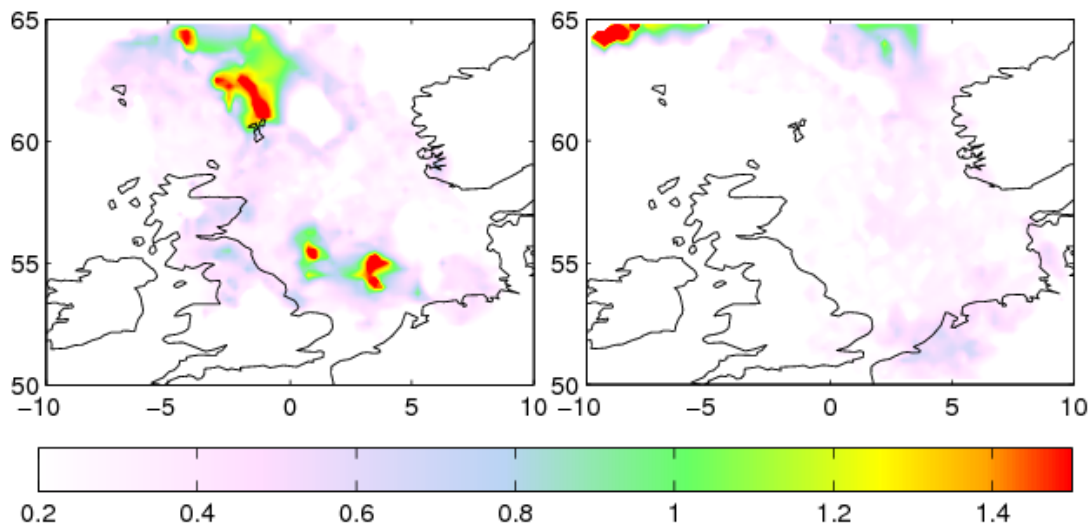


**Figure 7.** IASI ash mass loadings (in  $\text{g/m}^2$ ) on 17 May 2010. The morning orbit (left) includes data around 09:48 and 11:28 UTC, while the evening orbit (right) includes overpasses near 19:37 and 21:17 UTC.

In Figure 8 (a, b) IASI retrievals of ash mass column loading for morning and evening overpasses respectively are compared with those derived from lidar backscatter returns within the displaced selected area. In these plots the ash particles have been assumed to be spheres in the lidar derivation. Considering the uncertainties involved in both the IASI and lidar mass retrievals the level of agreement between the two sets of histograms is encouraging. For the IASI morning orbit some FOVs give relatively high ( $> 1.0\text{ g/m}^2$ ) mass retrievals which are not replicated in the lidar results. For the evening orbit the histograms show a greater degree of overlap.

The sensitivity of the lidar mass estimates to assumed particle shape is investigated in Figure 8 (c, d) where the lidar column mass has now been derived assuming the irregular particle model. Treating ash particles as irregular shapes rather than spheres decreases the lidar derived mass by around 30% for this flight (see Marengo et al. (2011)). Qualitatively, in the case of the IASI evening overpass the agreement with the lidar data is enhanced by using the non-spherical model, while for the morning overpass some outliers remain.

Given the uncertainties in tracking the ash cloud in the SEVIRI imagery, and the possibility of temporal variations in the ash density, the agreement of IASI and lidar mass estimates in Figure 8, based on observations separated in time by several hours, is rather good. Further corroboration of the IASI mass retrievals comes from the in situ data analysis of Turnbull et al. (2012) for this case study: for four profiles (ascents and descents) through the ash layer the column ash loading estimated from FAAM CAS measurements (default irregular model) was between 0.22-0.71  $\text{g/m}^2$ . Coterminous measurements with the nephelometer scattering probe produced estimates of 0.29-0.72  $\text{g/m}^2$ . These values are entirely consistent with the lidar and IASI histograms presented in Figure 8. Taken together, these results represent a credible validation of the IASI aerosol retrieval algorithm.

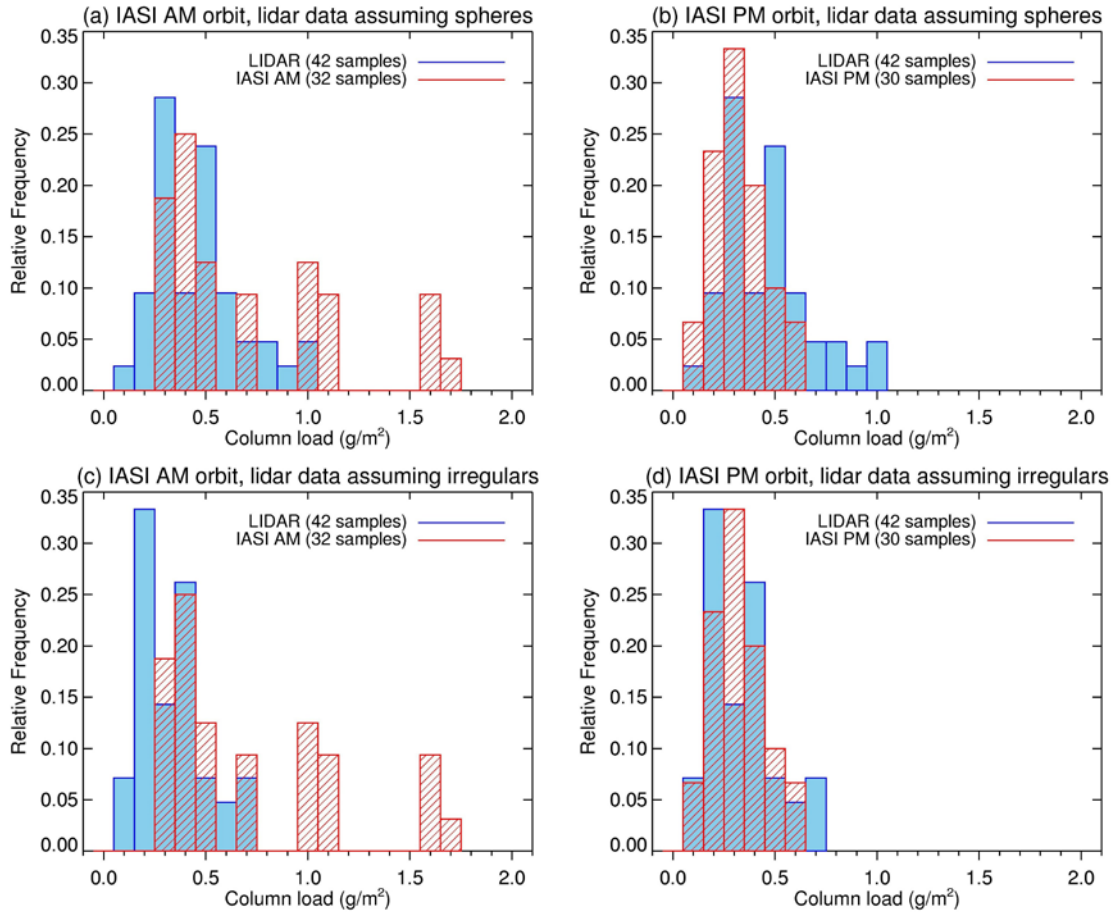


**Figure 8.** Histogram comparison of aerosol mass column loading retrievals from IASI (hatched bins) and FAAM BAe 146 lidar (filled bins). (a) Mass loadings corresponding to IASI morning orbit on 17 May 2011, lidar estimates based on assumption of spherical particles. (b) Mass loadings for IASI evening orbit, lidar estimates based on spheres. (c, d) As (a, b) but lidar estimates based on assumption of irregularly shaped particle model.

## 5. Conclusions

The Eyjafjallajökull eruption afforded a valuable opportunity to determine in situ properties of volcanic ash in conjunction with lidar backscatter measurements and observations of longwave and shortwave radiation. We have focused here on measurements from 17 May 2010 where the ash cloud was advected over the southern North Sea in otherwise clear sky conditions. This presented an ideal case study, as the presence of water or ice cloud would have complicated our analysis considerably. We

believe the unique combination of instrumentation on the FAAM BAe 146 atmospheric research aircraft makes this a valuable data set with which to test our understanding of volcanic ash microphysical and radiative properties. Indeed, our experience of flying with this configuration during April-May 2010 was vital in influencing the choice of instrumentation for the dedicated Met Office Civil Contingency Aircraft (MOCCA), a twin piston engine Cessna, which became operational in 2012.

The sensitivity of infrared ARIES spectra to the presence of volcanic ash has been demonstrated, with a clear relationship between lidar AOD and brightness temperature signatures. Our results for a sophisticated retrieval algorithm for IASI show that it is possible to derive ash mass loadings in good agreement with those determined from the airborne lidar. The IASI mass estimates are also consistent with values derived from intercepts of the ash cloud with the FAAM BAe 146 using optical particle counter and nephelometer scattering measurements. To our knowledge this is the first independent verification of a hyperspectral aerosol retrieval scheme, and gives confidence in the ability to retrieve key parameters such as aerosol mass from infrared space-borne sounders.

The use of mineral dust refractive indices due to Balkanski et al. (2007) and aircraft measured PSD is shown to be successful in reproducing the spectral signature of ash from this eruption across the infrared (8-13  $\mu\text{m}$ ) spectral range. While the use of Balkanski et al. (2007) refractive indices has led to the optimal agreement in this specific case, we acknowledge that the refractive indices of the volcanic plume from Eyjafjallajökull may change significantly during the course of the eruption as evidenced by the airborne measurements made by Schumann et al. (2011). Remarkably, their data show a very high proportion of large ( $> 1 \mu\text{m}$ ) particles were composed of silicates on the date of this case study (17 May 2010), which was not the case two weeks earlier on 2 May 2010 (see Figure 9, reproduced from their paper). Since the larger particles are expected to have most radiative impact in the longwave infrared region this offers support for our use of a mineral dust refractive index in this work.

This complexity in terms of refractive index is an obvious barrier to satellite retrievals, but the use of high spectral resolution instrumentation such as the aircraft-borne ARIES and satellite-borne IASI sensors in minimizing modeled and measured spectral differences shows some promise. The ash optical properties are known to be acutely sensitive to the characteristic ash composition for each eruption, particularly in terms of the aerosol refractive index and PSD. This motivates the need for a better understanding of the variability of volcanic ash mineralogy and improved measurements of refractive indices in future.

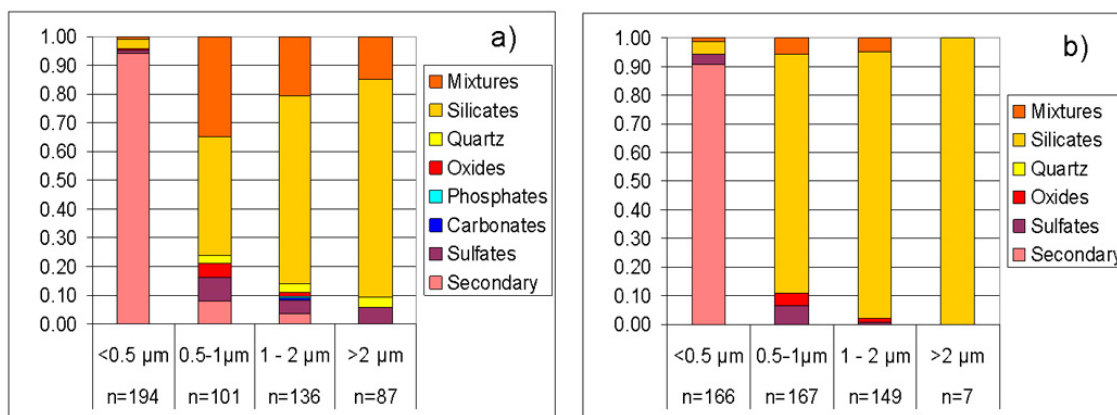


**Figure 9.** Relative number abundance of collected particles differentiated by size bin;  $n$  is the total number of particles analyzed per bin. Different chemical compositions are represented by different colors in the plot, see legend. Data are shown (a) for 2 May 2010, (b) for 17 May 2010. Figure reproduced from Schumann et al. (2011), see their paper for more details.

## Acknowledgments

Airborne data were obtained using the BAe 146-301 Atmospheric Research Aircraft (ARA) flown by Directflight Ltd and managed by the Facility for Airborne Atmospheric Measurements (FAAM), which is a joint entity of the Natural Environment Research Council (NERC) and the Met Office. The CAPS instrument was provided through the Facility for Ground-based Atmospheric Measurement (FGAM) by Martin Gallagher, Hugh Coe and James Dorsey at the Centre for Atmospheric Science, University of Manchester. IASI has been developed and built under the responsibility of the Centre National d'Etudes Spatiales (CNES, France). It is flown onboard the Metop satellites as part of the EUMETSAT Polar System. The IASI L1 data are received through the EUMETCast near real time data distribution service. L. Clarisse is Postdoctoral Researcher with F.R.S.-FNRS.

## Main reference

Newman, S. M., L. Clarisse, D. Hurtmans, F. Marengo, B. Johnson, K. Turnbull, S. Havemann, A. J. Baran, D. O'Sullivan, and J. Haywood (2012), A case study of observations of volcanic ash from the Eyjafjallajökull eruption: 2. Airborne and satellite radiative measurements, *J. Geophys. Res.*, 117, D00U13, doi:10.1029/2011JD016780.

## All references

Balkanski, Y.; Schulz, M.; Claquin, T. & Guibert, S. Reevaluation of Mineral aerosol radiative forcings suggests a better agreement with satellite and AERONET data. *Atmospheric Chemistry and Physics*, 2007, 7, 81-95.

Clarisse, L.; Hurtmans, D.; Prata, A. J.; Karagulian, F.; Clerbaux, C.; Mazière, M. D. & Coheur, P.-F., Retrieving radius, concentration, optical depth, and mass of different types of aerosols from high-resolution infrared nadir spectra. *Appl. Opt.*, 2010a, 49, 3713-3722.

Clarisse, L.; Prata, F.; Lacour, J.-L.; Hurtmans, D.; Clerbaux, C. & Coheur, P.-F. A correlation method for volcanic ash detection using hyperspectral infrared measurements. *Geophys. Res. Lett.*, 2010b, 37, L19806.

Clerbaux, C.; Boynard, A.; Clarisse, L.; George, M.; Hadji-Lazaro, J.; Herbin, H.; Hurtmans, D.; Pommier, M.; Razavi, A.; Turquety, S.; Wespes, C. & Coheur, P.-F. Monitoring of atmospheric composition using the thermal infrared IASI/MetOp sounder. *Atmos. Chem. Phys.*, 2009, 9, 6041-6054.

DeSouza-Machado, S.; Strow, L.; Hannon, S. & Motteler, H. Infrared dust spectral signatures from AIRS. *Geophys. Res. Lett.*, 2006, 33, L03801.

Guffanti, M., T. J. Casadevall and K. Budding (2010), Encounters of aircraft with volcanic ash clouds: a compilation of known incidents, 1953-2009. U.S. Geological Survey Data Series 545, ver. 1.0, 12 p., plus 4 appendixes including the compilation database.

Havemann, S., and A. J. Baran (2001), Extension of T-matrix to scattering of electromagnetic plane waves by non-axisymmetric dielectric particles: Application to hexagonal cylinders, *J. Quant. Spectrosc. Radiat. Transfer*, 70, 139-158.

Havemann, S. (2006), The development of a fast radiative transfer model based on an Empirical Orthogonal Functions (EOF) technique - art. no. 64050M, in *Multispectral, Hyperspectral, and Ultraspectral Remote Sensing Technology, Techniques, and Applications*, edited by W. L. Smith, A. M. Larar, T. Aoki and R. Rattan, pp. M4050-M4050.

Havemann, S., J. C. Thelen, J. P. Taylor, and A. Keil (2008), The Havemann-Taylor Fast Radiative Transfer Code: Exact fast radiative transfer for scattering atmospheres using Principal Components (PCs), in *Current Problems in Atmospheric Radiation*, edited by T. Nakajima and M. A. Yamasoe, pp. 38-40.

Haywood, J. M., et al. (2010), Observations of the eruption of the Sarychev volcano and simulations using the HadGEM2 climate model, *J. Geophys. Res.*, 115, D21212, doi:10.1029/2010JD014447.

Johnson, B., K. Turnbull, J. Dorsey, A. Baran, Z. Ulanowski, E. Hesse, R. Cotton, P. Brown, R. Burgess, G. Capes, H. Webster, A. Woolley, P. Rosenberg and J. Haywood (2012), In-situ observations of volcanic ash clouds from the FAAM aircraft during the eruption of Eyjafjallajökull in 2010, *J. Geophys. Res.*, doi:10.1029/2011JD016760, in press.

Liu, X., W. L. Smith, D. K. Zhou, and A. Larar (2006), Principal component-based radiative transfer model for hyperspectral sensors: theoretical concept, *Applied Optics*, 45(1), 201-209.

Marengo F., B. Johnson, K. Turnbull, S. Newman, J. Haywood, H. Webster and H. Ricketts (2011), Airborne lidar observations of the 2010 Eyjafjallajökull volcanic ash plume, *J. Geophys. Res.*, 116, D00U05, doi:10.1029/2011JD016396.

Newman, S. M., L. Clarisse, D. Hurtmans, F. Marengo, B. Johnson, K. Turnbull, S. Havemann, A. J. Baran, D. O'Sullivan, and J. Haywood (2012), A case study of observations of volcanic ash from the Eyjafjallajökull eruption: 2. Airborne and satellite radiative measurements, *J. Geophys. Res.*, 117, D00U13, doi:10.1029/2011JD016780.

Patterson E.M. and C.O. Pollard, Optical properties of the ash from El Chichón volcano, *Geophys. Res. Lett.*, 1983, 10, 317-320.

Pavolonis, M. & Sieglaff, J. GOES-R Advanced Baseline Imager (ABI) Algorithm Theoretical Basis Document For Volcanic Ash (Detection and Height) 2009, [http://www.goes-r.gov/products/ATBDs/volcanic\\_ash.pdf](http://www.goes-r.gov/products/ATBDs/volcanic_ash.pdf)

Prata, A. J., G. Gangale, L. Clarisse, and F. Karagulian (2010), Ash and sulfur dioxide in the 2008 eruptions of Okmok and Kasatochi: Insights from high spectral resolution satellite measurements, *J. Geophys. Res.*, 115, D00L18, doi:10.1029/2009JD013556.

Pollack, J.; Toon, O. & Khare, B. Optical properties of some terrestrial rocks and glasses. *Icarus*, 1973, 19, 372-389.

Schumann, U., B. Weinzierl, O. Reitebuch, H. Schlager, A. Minikin, C. Forster, R. Baumann, T. Sailer, K. Graf, H. Mannstein, C. Voigt, S. Rahm, R. Simmet, M. Scheibe, M. Lichtenstern, R. Stock, H. Rüba, D. Schäuble, A. Tafferner, M. Rautenhaus, T. Gerz, H. Ziereis, M. Krautstrunk, C. Mallaun, J.-F. Gayet, K. Lieke, K. Kandler, M. Ebert, S. Weinbruch, A. Stohl, J. Gasteiger, S. Gross, V. Freudenthaler, M. Wiegner, A. Ansmann, M. Tesche, H. Olafsson, and K. Sturm (2011), Airborne observations of the Eyjafjalla volcano ash cloud over Europe during air space closure in April and May 2010, *Atmos. Chem Phys.*, 11, 2245-2279, doi:10.5194/acp-11-2245-2011.

Stohl, A.; Prata, A. J.; Eckhardt, S.; Clarisse, L.; Durant, A.; Henne, S.; Kristiansen, N. I.; Minikin, A.; Schumann, U.; Seibert, P.; Stebel, K.; Thomas, H. E.; Thorsteinsson, T.; Tørseth, K. & Weinzierl, B. Determination of time- and height-resolved volcanic ash emissions for quantitative ash dispersion modeling: the 2010 Eyjafjallajökull eruption *Atmospheric Chemistry and Physics Discussions*, 2011, 11, 5541-5588.

Turnbull, K.F., B.T. Johnson, F. Marengo., J.M. Haywood, U. Schumann, A. Minikin, B. Weinzierl, H. Schlager, S. Leadbetter and A. Woolley (2012), A case study of observations of volcanic ash from the

Eyjafjallajökull eruption: 1. In situ airborne observations, *J. Geophys. Res.*, 117, D00U12, doi:10.1029/2011JD016688.

Wilson, S. H. S., N. C. Atkinson, and J. A. Smith (1999), The development of an airborne infrared interferometer for meteorological sounding studies, *Journal of Atmospheric and Oceanic Technology*, 16(12), 1912-1927.

Witham, C. S., M. C. Hort, R. Potts, R. Servranckx, P. Husson and F. Bonnardot (2007), Comparison of VAAC atmospheric dispersion models using the 1 November 2004 Grimsvötn eruption, *Meteorol. App.*, 14, 27-38.